Pre-stack Seismic Inversion and AVO Analysis for Reservoir Characterization: a case study

Arcangelo G. Sena, Tad Smith, Veritas Exploration Services, Houston, Texas, USA*
Juan Soldo, Diego Lenge, Mario Sigismondi, Augusto Silva Telles, Pecom Energía S.A, Neuquén, Argentina

Abstract

The successful exploration for new reservoirs in mature areas, as well as the optimal development of existing fields, requires the integration of unconventional geological and geophysical techniques. In particular, the calibration of 3D seismic data to well log information is crucial to obtain a quantitative understanding of reservoir properties. The advent of new technology for prestack seismic data analysis and 3D visualization has resulted in improved fluid and lithology predictions prior to expensive drilling. Increased reservoir resolution has been achieved by combining seismic inversion with AVO analysis to minimize exploration risk.

In this paper we present an integrated and systematic approach to prospect evaluation in the María Inés Oeste field, Argentina. We will show how petrophysical analysis of well log data can be used as a feasibility tool to determine the fluid and lithology discrimination capabilities of AVO and inversion techniques. Then, a description of effective AVO and prestack inversion tools for reservoir property quantification will be discussed. Finally, the incorporation of the geological interpretation and the use of 3D visualization will be presented as a key integration tool for the discovery of new plays.

Geological framework

The María Inés sandstones represent the base of a Second Order Transgressive System Tract (TST), deposited in a coastal to open shelf environment. These sands represent a transgressive clastic depositional system in the Austral Foreland Basin. The discontinuity over which these sandstones were deposited represents one of the orogenic pulses of the Andean Orogeny. In a few wells located to the west and northwest of the area of study it is possible to define a lower sand body, which represents the Lowstand System Tract (LST), limited by incised valleys. To the east of the study area, the sandstones onlap the regional forebulge represented by an antiform with a north-south axis that plunges to the south.

The Maastrichtian – Paleocene sandstones are seismically well defined, due to their thickness (50 meter average) and hydrocarbon content. In the study area the traps are mainly structural, associated with an east-west normal fault system. As they are charged to the spillpoint, the faults themselves determine the amount of the hydrocarbon trapped. Seismically, the response to this combination is in the form of bright spots, limited at their northern edge by faults.

Petrophysical Analysis

The development of the María Inés field was essentially based on the detection of these bright spots and their structural evaluation using 3D seismic data. After drilling almost ten wells, a further investigation of these amplitude anomalies became necessary.

A petrophysical analysis was carried out to evaluate the various relationships between lithology and fluid type via trend analysis and cross-plotting techniques. This first-stage determined which petrophysical attribute, or combination of attributes, shows characteristics that can be used as an identifier of a specific lithology and pore fluid. This understanding provides a preliminary assessment on which AVO attribute products can be diagnostic.

Prior to AVO modeling, all wells were processed using standard log editing and interpretation techniques. Two of the wells used in this study had measured shear velocities. For those wells without shear velocities, a local estimator was developed and applied; care was taken to ensure that shear velocities across pay were properly calculated. Gassman's equation was used to replace the insitu fluid in each well with three different fluids. Thus, brine, gas and two oil cases were generated for each well evaluated. Figure 1 shows the interval of interest from one of the wells.

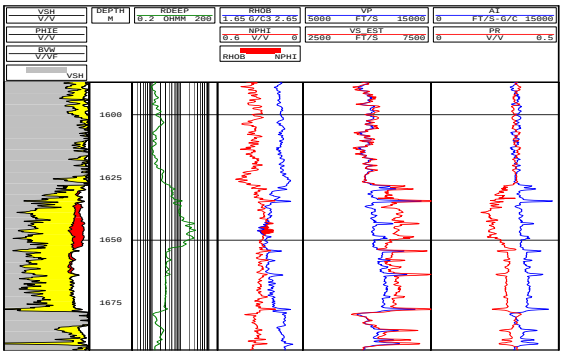

Figure 1.- Log display of one of the gas wells from the study area. Note the sharp contrast in acoustic impedance between the overlying shale and the sand.

Note that the top of the pay zone shows a gradational contact on Vshale and resistivity. However, examination of the acoustic impedance curve shows a sharp boundary at the top of the sand. This sharp interface was used to generate a simple reflectivity model (using Shuey's 3-term approximation, Figure 2).

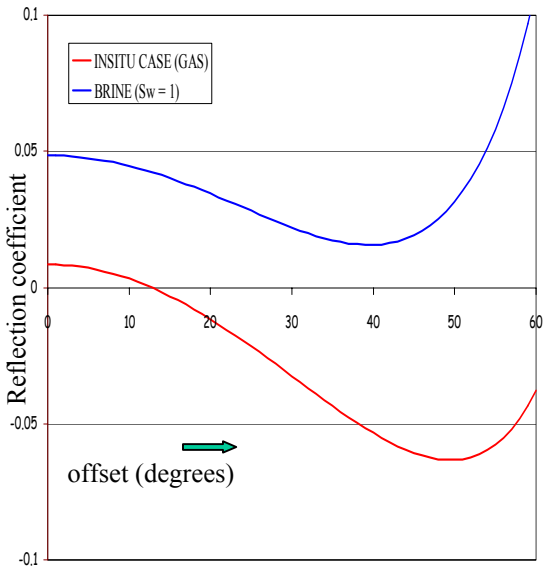

Figure 2.- Reflectivity model of the top reflector from the well shown in Figure 1. Shuey's 3-term approximation was used to generate this plot. Note that this well generates a Class II AVO response with a phase reversal at near offsets.

Note that the insitu response generates a strong Class II AVO response, with pronounced "brightening" in the far offsets. When the insitu fluid is replaced with brine, large changes in intercept, and small changes in gradient, are observed. Note, however, that no phase reversals are observed for the brine case. Although no appreciable changes in gradient are observed, the large changes in intercept cause this sand to be anomalous in intercept-gradient cross-plot space (Figure 3). Note from Figure 3, that under the model conditions evaluated in this study, there is little difference between the various hydrocarbon cases. The brine case, however, falls along a well-defined "background" trend.

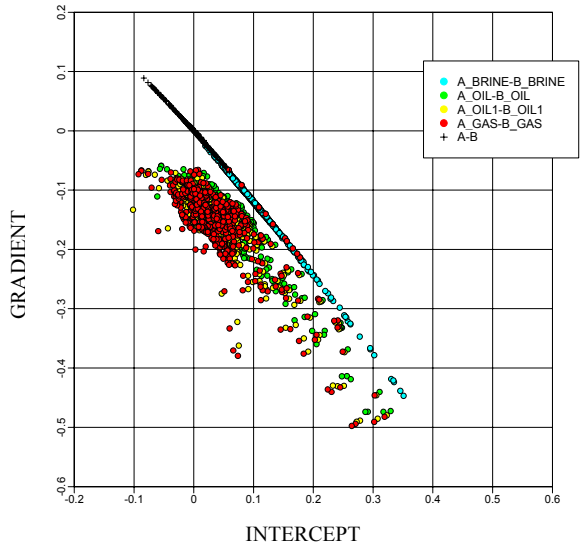

Figure 3.- Intercept-gradient cross-plot. Note that the shale and brine sands fall along a well-defined background trend, whereas the hydrocarbon cases are anomalous. Note, however, that intercept-gradient analysis will provide little leverage for discriminating the type of fluid in the reservoir.

Figure 4 is cross-plot of mu-rho ($\mu\rho$) vs. lambda-rho ($\lambda\rho$). As with standard intercept-gradient analysis, we observe separation between the brine and shale background trends and the hydrocarbon cases. Importantly, note that the amount of separation between the hydrocarbon cases and the brine case is more pronounced than in standard intercept-gradient format. Also note that additional separation may be observed between the different hydrocarbon cases using LMR techniques.

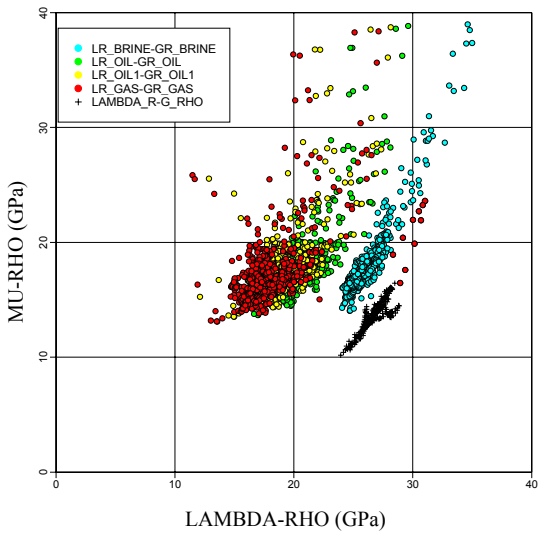

Figure 4. - Mu-rho vs. Lambda-rho cross-plot. As with intercept-gradient, shale and brine sands fall along a well defined background trend, whereas the hydrocarbon cases are anomalous, and nearly always have lambda-rho values less than 25 GPa. Note that brine sands have lambda-rho values greater than 25 GPa.

Geophysical Analysis

An AVO study, followed by prestack seismic inversion, was carried out over a specific area that included the producing zones and the potential future locations that resulted from the first interpretation.

The analysis involved the AVO attribute generation followed by prestack seismic inversion. Based on the results from the AVO modeling, the fluid factor attribute (Smith and Gidlow, 1987) volume was generated and a time slice at the zone of interest is shown in Figure 5. We can see the good correspondence between the strong fluid factor anomalies and the known hydrocarbon accumulations.

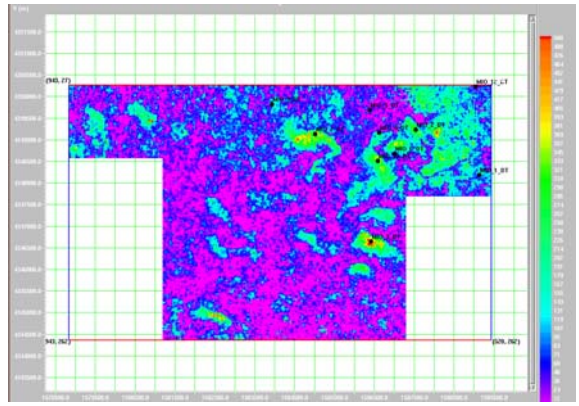

Figure 5.- Maximum value of fluid factor attribute within a 20 ms window below horizon of interest.

In order to combine the lithology/fluid discrimination capabilities of AVO analysis with the increased vertical resolution associated with seismic inversion we carried out prestack seismic inversion. The first step was to generate P- and S-wave reflectivity volumes via AVO analysis. Then we proceed to invert these volumes for acoustic and shear impedance. These impedance volumes can be combined to generate incompressibility times density ($\lambda\rho$) and rigidity times density ($\mu\rho$) volumes (Gray, 1999). The former attribute indicates changes in pore fluid content, while the latter is an indicator of lithology changes. In Figure 6, we show a crossplot of the seismically derived $\mu\rho$ vs $\lambda\rho$ at the well MIO-3 location. Red corresponds to gas, green to oil and blue to brine. The cross section corresponds to several CDPs around the well. We can see a clear delineation of the gas sand at this location

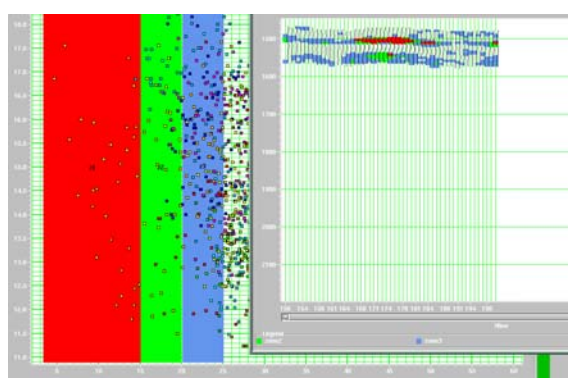

Figure 6.- Crossplot of $\mu\rho$ vs $\lambda\rho$ at well MIO-3 location. Red corresponds to gas, green to oil and blue to brine. The cross section corresponds to several CDPs around the well location.

In Figure 7 we show a λρ display from the 3D volume indicating the potential hydrocarbon areas. The color code shows green for oil and red for gas, according to the well calibration analysis indicated in Figures 4 and 6 for a typical well.

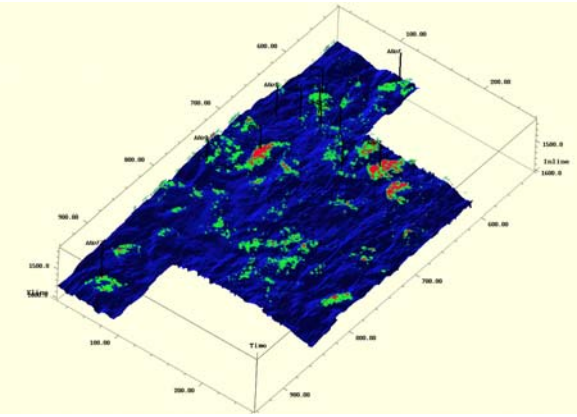

Figure 7.- 3D display of λρ volume over the María Inés Oeste field. New discovery well is MIO-12 to the westernmost part of the field. The color code shows green for oil and red for gas, according to the well calibration analysis in Figures 4 and 6.

The use of 3D visualization tools allowed combining the petrophysical, geological, and geophysical results for a faster interpretation of the area. After this study, additional wells were successfully drilled in the northwest and southwest parts of the area. Well MIO-12 was drilled on a λρ anomaly discovering a new play in an upper sandstone that belongs to the same TST. The calibration of seismic and well log data proved very successful in detecting new accumulations and more accurate areal extension of known plays.

Discussion and Conclusions

The systematic use of geological, petrophysical, geophysical and 3D visualization techniques have proven very effective in the development of existing fields. We have seen that the use of AVO in conjunction with seismic inversion combines the increased lithology/fluid discrimination of AVO with the augmented vertical resolution associated with the inversion procedure. Additional production from successful wells drilled in the area more than offset the technology cost in the María Inés Oeste field.

The proper calibration of seismic and well data together with the use of 3D visualization tools allowed to combine the petrophysical, geological, and geophysical results for a faster interpretation of the area. This approach has proven to be very effective in detecting new accumulations and a more accurate areal extension of known plays.

References

Smith, G. C. and Gidlow, P. M., 1987, Weighted stacking for rock property estimation and detection of gas: Geophys. Prosp., 35, no. 09, 993-1014.

Gray, F., Chen, T. and Goodway, W., 1999, Bridging the gap: Using AVO to detect changes in fundamental elastic constants: Annual Meeting Abstracts, Society Of Exploration Geophysicists, 852-855.

Acknowledgements

The authors gratefully acknowledge Pecom Energía management for permission to publish this paper.